



Research article

Variability in the substitution pattern of hydroxypropyl cellulose affects its physico-chemical properties

Gilles Cremer^{a,*}, Sabine Danthine^a, Vera Van Hoed^b, Anne Dombree^b, Anne-Sophie Laveaux^b, Christian Damblon^c, Romdhane Karoui^d, Christophe Blecker^a

^a Laboratory of Food Science and Formulation, GxABT, University of Liege, Belgium

^b Puratos NV, Groot-Bijgarden, Belgium

^c MolSys Research Unit, Faculty of Sciences, University of Liege, Belgium

^d Univ. Artois, Univ. Lille, Univ. Littoral Côte D'Opale, Univ. Picardie Jules Verne, Univ. of Liege, INRAE, Junia, UMR-T 1158, BioEcoAgro, F-62300, Lens, France



ARTICLE INFO

Keywords:

Cellulose ethers

Hydroxypropyl cellulose

Substitution pattern

Structure-function

ABSTRACT

Hydroxypropyl cellulose (HPC) is a water-soluble polymer with many applications in food, pharmaceutical, medical, or paints industries. Past studies have reported that differences in functionality can occur between products of similar pharmaceutical grades. Understanding the origin of these differences is a major challenge for the industry. In this work, the structure and physico-chemical properties of several HPC samples of the same commercial grade were studied. Structural analysis by NMR and enzymatic hydrolysis were performed to study molar substitution and distribution of substituents along the polymer chain respectively. Water-polymer interactions, surface properties as well as rheological and thermal behavior were characterized to tentatively correlate them with the structure, and gain new insights into the structure-function relationship of this polymer. The differences in structure revealed between the samples affect their properties. The unexpected behavior of one sample was attributed to a more heterogeneous substitution pattern, with the coexistence of highly and weakly substituted regions along the same polymer chain. The more block-like distribution of substituents has a great effect on the clouding behavior and surface tension reduction ability of the polymer.

1. Introduction

Hydroxypropyl cellulose (HPC) is a cellulose derivative in which some of the hydroxyl groups in the repeating glucose units have been hydroxypropylated. The resulting non-ionic polymer is soluble in water below its critical solution temperature and in many organic solvents [1]. The main features of HPC are its great surface properties [2] and its good film forming ability [3] compared to other cellulose ethers. Due to its unique properties, HPC has a wide range of industrial applications such as use in pharmaceutical tablets [4], ophthalmic inserts [5], smart windows [6], and as emulsifier/stabilizer in the food industry [7].

Like many other cellulose ethers, HPC is typically prepared by nucleophilic reaction of cellulose hydroxyl groups with electrophiles such as alkyl halides or epoxides [8]. The reaction is performed under heterogeneous conditions by a slurry process where cellulose is

* Corresponding author. Bat. ABT01 G8 - SMARTECH, Passage des deportes 2, 5030, Gembloux, Belgium
E-mail address: g.cremer@uliege.be (G. Cremer).

dissolved in aqueous sodium hydroxide, in the presence of an organic solvent [9]. Due to the flexibility of this manufacturing process, HPC can be obtained in several grades. The reaction rate as well as the number of substituents at positions 2, 3 and 6 is dependent on the alkali concentration [9]. Furthermore, the native cellulose materials greatly differ in structure depending on their origin [10], and the reaction with the electrophile tends to proceed faster in the amorphous regions than in the crystalline region [11]. As a result, cellulose ethers are thought to have an unbalanced distribution of substituents, with highly and poorly substituted regions existing on the same cellulose chain [12]. Commercial HPCs are typically characterized by average values of MW, hydroxypropoxy content (%), particle size, and viscosity, thus not accounting for the variability that may exist within the sample.

Some authors have already reported that differences in properties can occur between products formulated with hydroxypropylmethyl cellulose (HPMC) of similar pharmaceutical grades [13]. It was reported that HPMC with the same substitution and viscosity grade can have significantly different cloud points (CP) [14] or polymer release from matrix tablet [15,16]. HPC has received much less attention in the literature, but a study of Desai et al. suggests that such differences may also exist between HPCs of the same grade [17]. They studied the effect of HPC on the dissolution of pharmaceutical tablets and reported differences in performance between HPCs from different suppliers that both met the National Formulary criteria. These differences in properties between materials of same grade represent a challenge for the industry, and the current knowledge on this subject still contains many grey areas.

The distribution of substituents within the anhydroglucose unit and molecular chain is known to be an important parameter determining the physico-chemical behavior of cellulose derivatives in general [18]. The chain architecture affects the inter- and intramolecular hydrogen bonding formation, which impact a series of parameters such as solubility, crystallization, chemical reactions of hydroxyl groups [19] and gelation [20]. The knowledge about the impact of structure on the functionality of HPC has been increasing over the years. The influence of the molar substitution (MS) and MW is fairly well established. The relationships between MS and (i) the interaction with water and the equilibrium moisture content [21,22], (ii) the glass transition temperature [23], and (iii) the CP [22] were established a long time ago. The MW of the polymer is known to be positively correlated with the viscosity of aqueous solutions, and that shorter chain polymers (lower MW) show less shear thinning [7]. The impact of MW on surface tension (SFT) was also investigated [24]. The authors reported that MW has a significant effect on the adsorption kinetics at the interface; lower MW molecules decreased the SFT faster, which was attributed to their higher diffusion coefficient. On the other hand, the MW had little influence on the SFT at equilibrium. A link between the CP and the distribution of substituents along the polymer chain has been suggested by Schagerlöf et al. (2006) [25]. However, the consequences of differences in distribution of substituents along the polymer chain and the impact on important functional properties such as surface-activity, and rheological behavior has often been overlooked. Most studies investigating the link between structure and function have focused on HPC-water interactions [21,26,27] or dissolution from tablet [17,28]. Since the functionality of these polymers is largely dictated by their structure, a more detailed study of the structure-properties relationship is required. Accordingly, the aim of this paper was to identify the origin of these differences, as well as to provide a better understanding of the structure-function relationship of this polymer.

2. Experimental section

2.1. Materials

All HPC investigated met the same technical specifications: average MW: 620,000 Da, viscosity (2%, 25 °C): 200–400 mPa s, MS: 3.5–4.1. Microcrystalline cellulose Avicel® PH-101 (MCC) was used as reference material in powder X-ray diffraction and NMR analyses. HPC solutions were prepared by dispersing the required amount of HPC in ultrapure water (18.2 MΩ cm, RephiLe Bioscience) at room temperature. Solutions were kept under agitation for at least 2 h and stored overnight to ensure complete hydration before use.

2.2. Structural determination

2.2.1. Molar substitution

The MS was determined by proton nuclear magnetic resonance (¹H NMR). HPC samples were prepared by dissolving 15 mg of the product in 1 ml of 20% deuterium chloride (DCl). Samples were hydrolyzed at 50 °C for 96 h before measurements. The ¹H NMR spectra were recorded at 700 MHz using a Bruker Advance III HD instrument, equipped with a cryoprobe TCI. Substitution was calculated as follows:

$$MS = \frac{\int \text{CH}_3}{3 \int \Sigma \text{H}(1)} \quad (1)$$

2.2.2. Heterogeneity in substitution

The heterogeneity in the substitution pattern was determined by enzymatic hydrolysis followed by determination of reducing sugars (RS) content. The hydrolysis was carried out according to a method adapted from Viriden, Larsson, & Wittgren (2010) [29]. Samples were dissolved in 5 mM NaOAc (pH adjusted to 5.0) at a concentration of 1 mg/ml 20 U of endo-1,4-β-D-glucanase from *Trichoderma longibrachiatum* (Megazyme, Ireland) were added to 2 ml of samples. Hydrolysis was performed at 30 °C for 48 h, under constant stirring. RS determination following enzymatic hydrolysis was performed by the DNS assay according to a method adapted from Wood & Bhat (1988) [30]. 0.9 ml of DNS reagent was added to an aliquot of 0.3 ml of hydrolyzed samples. Solutions were filtered on 0.45 μm filter, and test tubes were placed in a boiling water bath for 5 min. Samples were cooled down to room temperature and absorbance was read at 540 nm. The blanks was the HPC solutions without enzymes. Calibration curve was established with glucose

between 0.05 and 0.6 mg/ml.

2.3. Powder characterization

2.3.1. Crystallinity

The crystallinity of the HPC powders was determined by powder X-ray diffraction using a Bruker D8-Advance Diffractometer coupled with a Lynxeye detector (Bruker, Germany). The diffractograms were recorded in the range of 2θ from 5 to 40° with 1128 steps and a time per step of 5 s. Crystallinity index (CI) was calculated by the peak height method adapted from Segal, Creely, Martin, & Conrad, (1959) [31]:

$$(I_{002} - I_{AM}) / I_{002} \times 100 \quad (2)$$

I_{002} = peak intensity from the (002) lattice plane ($2\theta = 20.2^\circ$ for HPC, 22.5° for MCC).

I_{AM} = peak intensity from amorphous phases ($2\theta = 12.0^\circ$ for HPC, 18.0° for MCC).

The d-spacings (d), representing the interplanar distances were calculated according to the Bragg equation:

$$n\lambda = 2d \sin \theta \quad (3)$$

n = an integer representing the diffraction order.

λ = wavelength of the X-ray

d = interplanar distance in the crystal lattice.

θ = the angle between incident ray and the scatter plane

2.3.2. Dynamic vapor sorption (DVS)

Moisture sorption isotherms were obtained using a DVS Advantage instrument (Surface measurements systems, United-Kingdom). Experiments were conducted at 25°C on a sample mass of approximately 100 mg. The device measures sample mass while controlling relative humidity (RH) in sample chamber. Relative humidity is controlled by modulations of two flows: saturated water vapor, and dry nitrogen. The relative humidity was changed in 3% steps from 0 to 30%, and in 10% steps from 30% to 90%. A measurement is also made at 95%. Both sorption and desorption have been measured. Equilibrium was assumed when there was a weight change of 0.002% over a period of 10 min.

2.3.3. Hydration rate

The hydration rate was estimated by the rate of development of solution viscosity. 1 wt% solutions were prepared by dispersing HPC in ultrapure water. The solutions were then kept under stirring at room temperature, and their viscosity was measured after different hydration times. Dynamic viscosity was measured at 25°C , shear rate = 1000 s^{-1} using a MCR302 rheometer (Anton Paar, Austria) equipped with a CP50/1 probe. Since the solution viscosity develops when the molecules are solubilized and hydrated properly, the measurement of viscosity over time can be used as a tool to evaluate the hydration rate. Hydration rate was calculated as follows:

$$\text{Hydration rate (\%)} = ((V_1 - V_0) / (V_{24} - V_0)) \times 100 \quad (4)$$

V_0 = viscosity of ultrapure water at 1000 s^{-1} (mPa s).

V_1 = viscosity of the solution after 1 h hydration at 1000 s^{-1} (mPa s).

V_{24} = viscosity of the solution after 24 h hydration at 1000 s^{-1} (mPa s).

2.4. Surface properties

2.4.1. Static surface tension

Static SFT measurements were performed according to the Wilhelmy plate method using a Tensimat Prolabo No. 3 (Prolabo, France). SFT was determined after a 30 min equilibration period from the force applied to the platinum plate. The accuracy of the instrument was checked by ensuring that a value of 72.0 mN/m was obtained for milliQ water.

2.4.2. Dynamic surface tension

The dynamic SFT of 0.20 wt% HPC aqueous solutions was measured at 25°C with two complementary devices. The SFT under very short adsorption times (from 0.010 to 10 s) was measured using a BP 100 bubble pressure tensiometer (Krüss, Germany), equipped with a 0.250 mm glass capillary. A DVT50 drop volume tensiometer (Krüss, Germany) was used to investigate SFT over a larger time scale (≈ 5 –250 s). The apparatus was equipped with a 250 μl syringe and a 2.986 mm diameter metal capillary. Equilibrium SFT was calculated from the values obtained from the last 5 drops by extrapolating the SFT to time $t \rightarrow \infty$ in the $\sigma - t^{1/2}$ curves [32].

2.4.3. Surface hydrophobicity

The surface hydrophobicity (SH) of HPC samples was assessed by fluorescence spectroscopy. HPC solutions were titrated using 8-anilinonaphthalene-1-sulfonic acid (ANS) as a hydrophobic probe. Small aliquots of ANS were successively added to 2 ml of 0.2 wt% HPC solutions to reach ANS concentration of 0, 20, 40, 60, 80, 100, and 120 μM . Samples were excited at 390 nm and emission spectra

were acquired from 400 to 650 nm with a FluoroMax-4 spectrofluorometer (Horiba Jobin Yvon, France). After titration, the binding parameters were established. F_{\max} corresponds to the maximum attainable fluorescence at saturating ANS concentration. It is an indication of the number of hydrophobic sites accessible to the spectroscopic marker [33]. K_d is the apparent dissociation constant of a supposedly monomolecular HPC-ANS complex. It corresponds to the ANS concentration required to reach $F_{\max}/2$ due to Michaelis–Menten kinetics [34]. The surface hydrophobicity was calculated as $SH = F_{\max}/K_d \cdot [HPC]$.

2.4.4. Surface dilatational rheology

An automated drop tensiometer (Tracker, Teclis Scientific, France) was used to investigate the influence of HPC on interfacial rheology. A 5 μ l air bubble was created in the surrounding HPC solution using a U-shaped capillary. The evolution of SFT over time was followed by drop shape analysis. A steady state was assumed after 15 min, and sinusoidal deformation with a volume amplitude of 10% and a frequency of 0.1 Hz was applied to the bubble for 100 s. The SFT (σ) was recorded against surface area (A), and the dilatational surface modulus (E) was determined as $E = d\sigma/dA$. Measurements were carried out at 25 °C.

2.5. Rheological behavior

Rotational viscosity analysis was carried out using a MCR302 rheometer (Anton Paar, Austria) equipped with a Peltier temperature control system. The instrument operated in a cone-plate geometry, with a CP50/1 probe (50 mm diameter, cone angle of 1°, and gap of 0.102 mm). Measurements were performed at 25 °C and samples were rested for 5 min before analysis to allow temperature equilibration. Shear rate was increased with a linear ramp from 0 to 1000 s^{-1} . The rheological data of the solutions was modeled according to the Herschel-Bulkley model:

$$\tau = \tau_0 + k \dot{\gamma}^n \quad (5)$$

τ = shear stress (Pa).

τ_0 = yield stress (Pa).

k = consistency index ($Pa \cdot s^n$).

$\dot{\gamma}$ = shear rate (s^{-1}), n = flow index (dimensionless).

2.6. Cloud point

The CP of the polymer was determined by light transmittance analysis using a UV–vis spectrophotometer (Hitachi U 2900, Tokyo Japan). Polymer solutions (0.1 wt%) were heated from 35 to 55 °C, at a heating rate of 0.2 °C/min, and the transmittance was measured at $\lambda = 600$ nm. The CP was determined as the temperature at which the transmittance was reduced to a value of 95%.

3. Results and discussion

A total of 6 HPC samples were considered. These samples were discriminated based on their static SFT, CP from suppliers, and the relationship between these two parameters (Fig. 1). Two groups of HPC could be distinguished: HPC#1, #2 and #6 had a low SFT associated with a low CP, and HPC#3 and #4 had a higher SFT with a higher CP. The correlation between static SFT and CP based on these 5 samples was very good ($R^2 = 0.991$). Surprisingly, one sample (HPC#5) deviated from this relationship. These preliminary results highlights that the relationship between the surface-activity of an HPC and its CP is not so straightforward, which emphasizes the relevance of a more detailed study. Three samples with distinct properties, namely HPC#1, #3, and #5 were selected for further analysis. An analysis of the structure of these samples was performed, and their properties were determined in more depth in order to possibly correlate the structure to the functionality of these molecules.

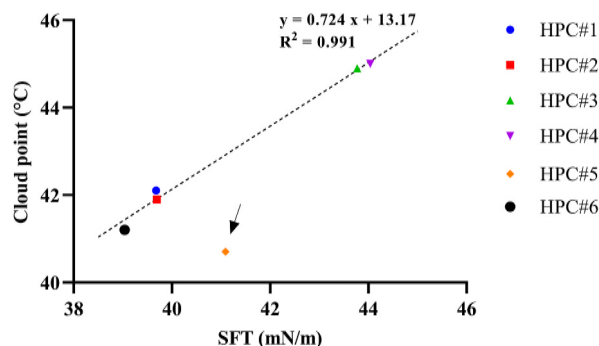


Fig. 1. Cloud point of HPC samples as a function of their static surface tension (25 °C).

3.1. Structural determination

3.1.1. Number/position of the substituents

^1H NMR and two-dimensional NMR experiments (edited HSQC) were performed to gain structural information. Edited HSQC allows the discrimination of CH_2 from CH/CH_3 . Since the methyl groups come only from the hydroxypropyl chains, the abundance of substituents is determined by comparing the CH_3/H_1 ratio using Eq. (1). The ^1H NMR spectra of HPC#1, HPC#3, and HPC#5 are displayed in Fig. 2A, B, and 2C respectively. The spectrum of MCC was determined for comparison (Fig. S1). The substitution was evidenced by the decrease of the intensity of the anomeric protons peaks, the increase of the intensity of the peaks in the H (2–6) region, as well as the appearance of an intense peak, corresponding to CH_3 . The methyl groups appeared as doublet at 0.96 ppm. The C1 cellulose protons appeared as two groups of peaks, corresponding to the two anomeric forms at 4.35–4.60 (H-1(β)) and 4.90–5.30 ppm (H-1($\alpha\text{MS} = 3.5\text{--}4.1$). However, similar values have already been reported by Fettaka et al. (2011) when determining the MS with the same analytical technique (^1H NMR) [35]. Heteronuclear single quantum coherence experiments ($1\text{H}\text{--}^{13}\text{C}$ HSQC) were also performed to gain insight into proton-carbon single bond correlations (Fig. S2). The CH_2OH signals that were visible in the MCC spectrum were no longer visible in the HPC samples, but different $\text{CH}_2\text{O-R}$ signals appeared, indicating a high degree of substitution. In the meantime, the CHOH signals in HPCs were shifted compared to the cellulose; it is thus very likely that the modification also concerns the CHOH , not only the CH_2OH . This observation indicates that several substituents are grafted at each position, which is in line with their large molar substitution.

3.1.2. Heterogeneity in substitution

It has been previously demonstrated that the ability of specific enzyme to degrade cellulose ethers is dependent on the substitution pattern. This technique has already been applied successfully to HPC [25] as well as to other cellulose ethers such as methylcellulose [36] and hydroxypropylmethyl cellulose [14]. The presence of substituents cause steric hindrance which prevent the enzyme to bind to the catalytic site on the anhydroglucose unit [37]. The amount of RS released after the hydrolysis greatly differed for the three samples, which reflected important differences in terms of enzymatic degradation. HPC#1 was most weakly degraded by the enzyme, releasing a very small amount of RS (0.087 ± 0.002 mg/ml). HPC#3 experienced a somewhat higher degradation, producing a slightly higher amount of RS (0.119 ± 0.003 mg/ml). This is likely to be due to its slightly lower amount of substituents. HPC#5 exhibited the highest amount of RS after enzymatic hydrolysis (0.206 ± 0.004 mg/ml). It released almost twice as much RS as the others, while having the lowest MS, which suggest that the substitution pattern is more heterogeneous in HPC#5. It could combine highly substituted and low substituted regions. The enzymatic degradation would proceed to a larger extent in the low substituted regions, therefore yielding a higher amount of RS. A representation of the presumed structure of the three samples studied is shown in Fig. 3.

3.2. Physico-chemical characterization

3.2.1. Powder properties

3.2.1.1. Crystallinity. The crystallinity was investigated to provide data about the order of molecular arrangement in the powder particle matrices. It is known that the solubility of HPC is facilitated by their low crystallinity [21]; a greater crystallinity generally implies a greater expenditure energy for the disruption of polymer-polymer interactions [38]. Crystallinity of HPC powders was investigated by powder X-ray diffraction (XRD) and diffraction patterns are presented in Fig. 4. XRD pattern of MCC was determined for comparison purpose (Fig. S3). It contained three well resolved peaks, located at 2θ angles of 16° , 22.5° , and 34.5° , which is consistent with values reported in the literature [39]. HPC samples were characterized by two broader diffraction peaks; the first one located around 8° and the second one, more intense, appeared at 20.3° , which indicated that HPCs were at least partially crystalline.

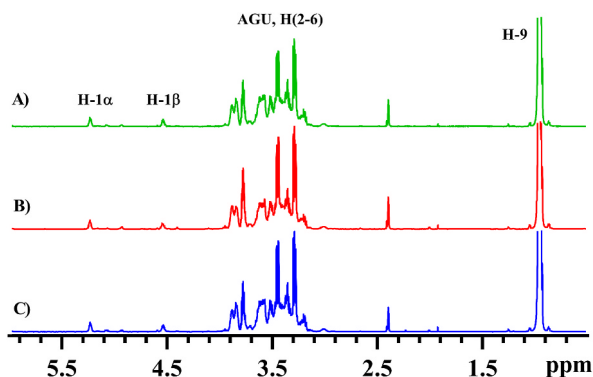


Fig. 2. ^1H NMR spectra of HPC#1 (A), HPC#3 (B), and HPC#5 (C) in 20% DCl at 25 °C.

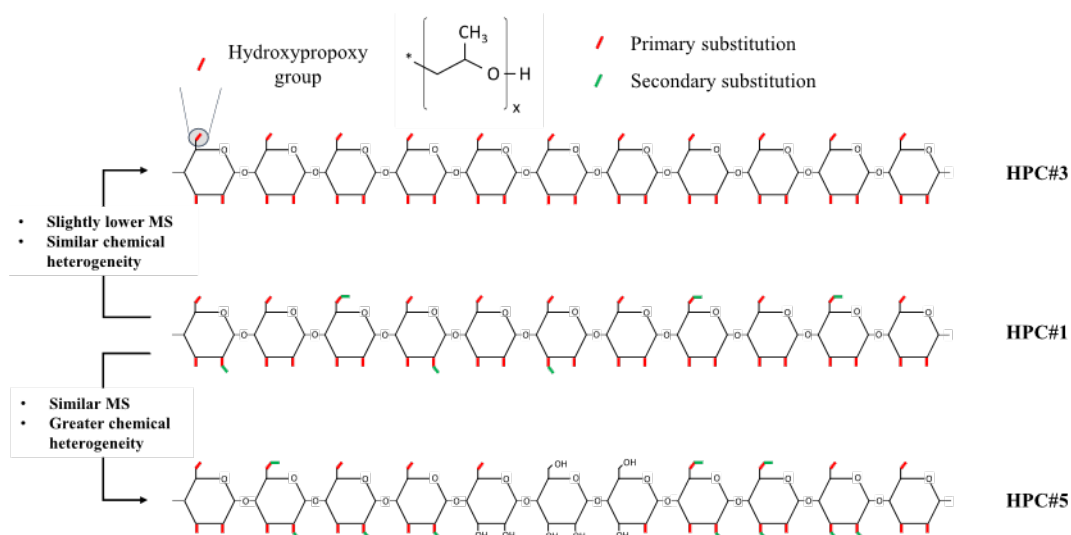


Fig. 3. Assumed structures for HPC#1, HPC#3, and HPC#5.

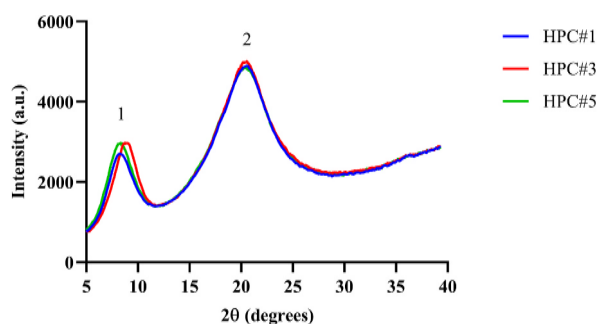


Fig. 4. X-ray diffractograms of HPC samples (20 °C).

The peak initially visible at 34.5° in the MCC is no longer visible in the HPC samples. Similar diffraction spectra were found by Talukder, Reed, Dürig, & Hussain (2011) [40]. CI were calculated using the peak height method as described by Eq. (2). As expected, MCC was highly crystalline with a CI of $87.6 \pm 0.2\%$. The HPC samples display lower crystallinity than the MCC, with CI of about 71% for the three samples.

The peak height method developed by Segal and coworkers is widely used to calculate crystallinity and compare the relative differences between cellulose samples. However this method does not account for the slight shift observed in the position of the first peak between samples. The position and d-spacings of each of the two peaks are shown in Table 1. The d-spacings were calculated following Eq. (3). The diffraction peak at $2\theta = 20^\circ$ was previously attributed to the slightly ordered amorphous phase of HPC while the peak at $2\theta = 9^\circ$ was attributed to the backbone-backbone d-spacing of the main chains in the crystalline phase of HPC [41]. The reaction of propylene oxide with reaction of hydroxyl groups of cellulose was shown to expand the d-spacing of the (110) plane [42]. These results are in line with the MS values, as determined by NMR. The slightly but significantly lower d-spacings observed for Peak 1 in the diffraction spectra of HPC#3 indicates a less pronounced substitution.

Our results show that the substitution of cellulose leads to a broadening of the two main diffraction peaks, and a shift of the first peak to lower angle 2θ values, with a corresponding decrease in the crystallinity of the polymer, in agreement with previous findings

Table 1
X-ray diffraction data for HPC#1, #3 and #5.

		HPC#1	HPC#3	HPC#5
Crystallinity index (%)		71.0 ± 0.8	71.4 ± 0.5	71.4 ± 0.5
Peak 1	2 theta ($^\circ$)	8.09 ± 0.05^a	8.62 ± 0.04^b	8.16 ± 0.01^a
	d-spacings (\AA)	10.92 ± 0.07^a	10.26 ± 0.04^b	10.82 ± 0.02^a
Peak 2	2 theta ($^\circ$)	20.29 ± 0.04	20.27 ± 0.01	20.27 ± 0.03
	d-spacings (\AA)	4.37 ± 0.01	4.38 ± 0.01	4.38 ± 0.01

Within the same line, means with different letters are significantly different at $P \leq 0.05$.

[43]. These results suggest that X-ray diffraction is sensitive to small variations in MS, and could be an interesting technique to compare MS between samples, by performing a measurement directly on the powder.

3.2.2. Dynamic vapor sorption (DVS)

Fig. 5 illustrates the sorption-desorption isotherms for the 3 different HPC samples. Few differences were observed between the HPC samples during the sorption phase. All three samples had profiles corresponding to Brunauer Type III isotherms. The samples behaved in the same way until they reached 90% RH. The curves can be divided into two regions: from 0 to 70% RH, the change in mass increased gradually, indicating a progressive adsorption of water molecules, and from 70% RH, the change in mass increased steeply. Slight differences appeared at 95% RH; at this humidity, the mass change of HPC#5 (34.4%) was slightly lower than that of HPC#1 (36.0%) and HPC#3 (37.1%), indicating that it had adsorbed less water.

Despite the similarities during the sorption phase, the samples behaved differently during the desorption phase. A hysteresis is observed for the three samples, and it is the most pronounced for HPC#3 (Fig. 5B) compared to HPC#1 (Fig. 5A) and HPC#5 (Fig. 5C). During desorption, HPC#3 had a higher mass change than the other two HPCs over the entire RH range. This indicates that the water adsorbed during the sorption phase was bound more strongly, and was therefore more difficult to desorb. The chain architecture has a strong influence on the structuring of water; differences in polysaccharide structure result in different spatially confined environments for water sorption [44]. It was previously demonstrated that the lower substituted HPCs had better capacity to bind water vapor internally [21]. This was attributed to their greater crystallinity and smaller degree of substitution. Substitution has a great impact on water adsorption as the capacity for monolayer adsorption is related to the ability of water to interact with hydrophilic groups of the substituents [45].

3.2.3. Hydration rate

In order to compare the hydration kinetics, the viscosity of HPC solutions was measured after 1 h and 24 h of hydration, and

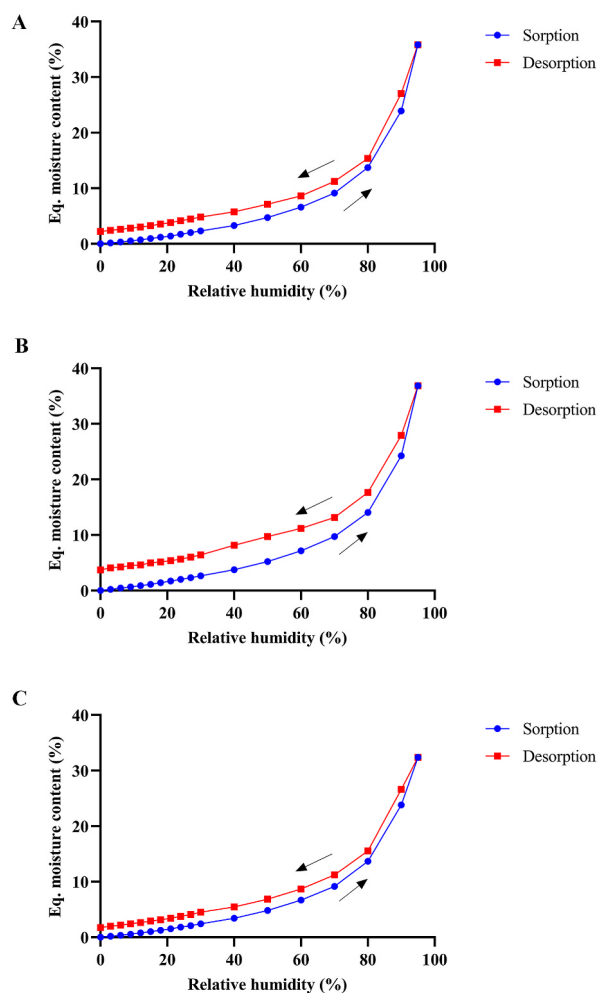


Fig. 5. Water sorption and desorption isotherms (25 °C) of: (A) HPC#1, (B) HPC#3, and (C) HPC#5.

hydration rates were calculated as described by Eq. (4). Major differences in the hydration kinetics of the samples were observed. HPC#5 was the fastest hydrating sample, with a hydration rate of $94 \pm 2\%$. HPC#1 hydrated slightly more slowly, with a hydration rate of $83 \pm 1\%$, and HPC#3 displayed the slowest hydration kinetics with a hydration rate worth $57 \pm 14\%$. These differences could be explained in term of differences in water affinity. Visually, it could be seen that HPC#3 was not properly dispersed after 1 h, and lumps formation was reported. The greater hydrophobicity of HPC#3 suggested by the DVS experiment would explain the lower hydration rate. Due to their higher affinity for water, HPC#3 molecules could quickly swell in contact with water, forming lumps, and preventing a good diffusion of water molecules towards the polymer core. This would result in a longer time to complete hydration.

3.2.4. Interfacial properties

The three HPC samples investigated were selected for further characterization based on a static SFT value. In order to gain a more comprehensive understanding of their interfacial properties, SFT was studied under dynamic conditions, and interfacial rheology was investigated as well.

3.2.5. Surface tension

a) Short term adsorption kinetics

The hydrophilic character of the cellulose backbone, combined with the more hydrophobic character of the substituent chains, gives HPC good surface properties. The evolution of SFT of HPC solutions as a function of surface age is depicted at Fig. 6. All three samples displayed quite similar adsorption kinetics. It has been previously reported that the adsorption of HPC at the interface is a three-step process, and the relative duration of each step depends on the concentration [2]. At the concentration investigated here, i.e. 0.2 wt%, no lag time is observed. The initial SFT were already substantially reduced at initial adsorption time (10 ms), highlighting the ability of these molecules to diffuse and adsorb rapidly at the interface. The progressive adsorption of molecules at the interface then resulted in a significant decrease of the SFT, up to values of approximately 45 mN/m for HPC#1 and #5, and 47 mN/m for HPC#3. This experiment shows that the three samples have similar adsorption kinetics. HPC#3, however, seems slightly less surface-active than HPC#1 and #5, as evidenced by its slightly higher SFT.

b) Long term adsorption kinetics

Measurements from the drop volume tensiometer allowed the study of adsorption kinetics over a longer time scale, and the extrapolation of SFT value at equilibrium. The evolution of SFT as a function of time is presented at Fig. S4. The equilibrium SFT of 0.2 wt% HPC solutions measured at 25 °C are as follows: HPC#1 had the lowest value (40.17 ± 0.07 mN/m), HPC#3 the highest (43.90 ± 0.01 mN/m), and HPC#5 had an intermediate value (40.80 ± 0.01 mN/m). The higher SFT values for HPC#3 revealed by the two measurement methods indicate that this HPC is less surface-active than the two others.

3.2.6. Surface hydrophobicity

Surface hydrophobicity was determined by fluorescence spectroscopy with ANS as a hydrophobic probe. The binding parameters between HPC and ANS were calculated and are presented in Table 2. Titration curves can be visualized in Fig. S5. The results indicate that the maximum fluorescence F_{\max} was significantly lower for HPC#3 compared to the other two. The apparent dissociation constant K_d was relatively similar for all HPC samples. The highest surface hydrophobicity was observed for HPC#5, although the difference with HPC#1 was not significant. HPC#3 had a significantly lower surface hydrophobicity than the other two.

A strong correlation was observed between the surface hydrophobicity and the hydration rate: an increase in surface hydrophobicity was associated with a faster hydration rate. More hydrophilic polymers would have a greater tendency to form viscous clusters during aqueous dispersion. This would hinder the diffusion of water towards the polymer core, resulting in slower hydration kinetics.

3.2.6.1. Dilatational rheology at the A/W interface. The dilatational rheology is known to play an important role in short-term stability

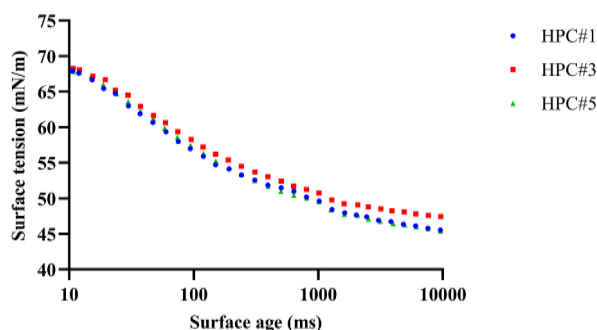


Fig. 6. Dynamic surface tension of 0.20 wt% HPC solutions as a function of surface age: HPC#1 (●), HPC#3 (■), HPC#5 (▲) (25 °C).

Table 2
Surface hydrophobicity parameters for HPC samples.

	HPC#1	HPC#3	HPC#5
F_{\max} (a.u.)	540.84 ± 3.64^b	503.44 ± 1.94^a	534.41 ± 2.44^b
K_d (μM^{-1})	20.62 ± 0.71^{ab}	21.03 ± 0.26^b	19.54 ± 0.59^a
Surface hydrophobicity	8.47 ± 0.24^b	7.72 ± 0.12^a	8.83 ± 0.22^b

F_{\max} : maximum fluorescence intensity; K_d : apparent dissociation constant. Within the same line, means with different letters are significantly different at $P \leq 0.05$.

of dispersions and can help to monitor the interfacial structure of surfactant [46]. The adsorption of surface-active species at the interface generates a gel-like network with elastic properties [47]. Dilatational rheology experiments were performed to compare the dilatational moduli of HPC samples. Significant differences were observed between the three samples (Table 3). HPC#1 had the lowest dilatational moduli. HPC#3 was characterized by slightly higher values, suggesting that the molar substitution had only a limited effect on the viscoelastic properties of the interface stabilized by HPC. On the contrary, HPC#5 was characterized by a significant increase in dilatational moduli, and by a slightly higher phase angle θ . The phase angle refers to the phase difference between SFT and the interfacial area variations. A higher value reflects a greater contribution of the viscous components to the dilatational modulus. The greater mechanical strength of interfacial layers stabilized by HPC#5 suggests that a stronger intermolecular network was formed at the interface. The adsorption of surface-active polymer at the interface is often described with the train-loops-tails model. The more polarized distribution of substituents along the polymer chain in HPC#5 would favor a more efficient exposition of hydrophobic regions at the interface. The higher protrusion length of the hydrophilic regions in the bulk would favor polymer-polymer interactions (see arrows in Fig. 7), and result in the formation of a more cohesive interfacial layer.

3.2.7. Flow behavior

Like many polysaccharides, HPC has a thickening effect in solution, which imparts colloidal stabilization [8]. Being an important functional property of the polymer, the study of the influence of HPC on the rheology is of prime importance for many applications. The flow behavior of HPC solutions is represented at Fig. 8 and the parameters of the Herschel–Bulkley model (see Eq. (5)) are found in Table 4. Since the shear stress τ_0 was null for all samples (Fig. 8A) this model reduced to a power law, with a good fitting for the three samples. All three have demonstrated a shear-thinning behavior, as indicated by their flow index $n < 1$; the viscosity was maximum at zero shear rate and progressively decreased as the shear rate increased (Fig. 8B). The viscosity of these aqueous solutions showed no thixotropy as indicated by the independence of the viscosity over time at constant shear, and by the absence of hysteresis between forward and backward curves (Figs. S6 and 7), in agreement with data available in the literature [48]. HPC#3 had the highest viscosity in the entire shear rate range studied, and was characterized by a slightly higher consistency index k , and higher flow index n compared to HPC#1 and HPC#5. Results emphasize that the rheological behavior of HPC solutions are sensitive to the MS of the polymer. The higher hydrophilicity of lower substituted HPCs would increase the water-polymer interactions, favoring a more extended conformation of the polymer, resulting in an increased viscosity. The substitution heterogeneity observed for HPC#5, on the contrary, does not significantly impact the rheological properties of the polymer at 25 °C.

3.2.8. Clouding behavior

HPC is a thermo-responsive polymer and undergoes a phase separation from solution above a certain temperature, namely lower critical solution temperature (LCST). For the purpose of investigating the structural changes of polymers during heating, the evolution of transmittance was recorded during heating from 35 °C to 55 °C and is presented in Fig. 9. The appearance of cloudiness during heating is detected by the transmittance measurement, and allows the detection of the CP. Different behaviors were observed and the shape of the curves and the CP are consistent with findings of Schagerlöf et al. (2006) [25]. The samples had CP values of 43.6, 46.1 and 41.6 °C for HPC#1, #3 and #5 respectively. HPC#3 stood out as having the highest cloud point. These values are slightly higher than those provided by the suppliers, which can be explained by the lower concentration of the solutions used for the measurements. Beyond the CP value, the samples differed by the shape of their curves. While HPC #1 and #3 were characterized by an abrupt decrease in transmittance beyond the CP, HPC #5 had a two-step clouding curve (see arrow Fig. 9). Since the onset of cloudiness at LCST is accompanied by a sharp drop in viscosity, rheometer can be used to estimate the CP as well [49,50]. The bimodal clouding behavior was also observed with a rheometer, when measuring the viscosity of HPC solutions during heating from 35 to 50 °C (Fig. S8). The broader clouding behavior in HPC#5 is thought to be driven by its uneven distribution of substituents along the chain. The more substituted regions would have a higher tendency to aggregate upon heating, resulting in a lower CP, while the less substituted regions

Table 3
Dilatational viscoelastic parameters of A/W interfaces stabilized with HPC.

	HPC#1	HPC#3	HPC#5
Dilatational elastic modulus E' (mN/m)	4.75 ± 0.02^a	5.17 ± 0.23^b	6.76 ± 0.26^c
Dilatational loss modulus E'' (mN/m)	0.77 ± 0.09^a	0.92 ± 0.07^a	1.47 ± 0.15^b
Phase angle θ (°)	9.28 ± 1.03^a	10.10 ± 0.30^a	12.25 ± 1.36^b

Within the same line, means with different letters are significantly different at $P \leq 0.05$.

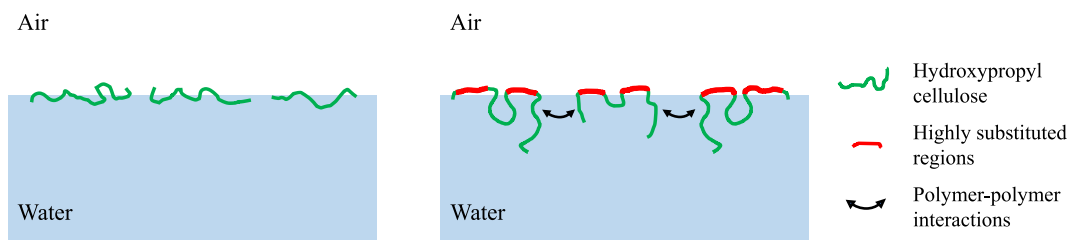


Fig. 7. Schematic representation of adsorption of homogeneously substituted HPC (left), and heterogeneously substituted HPC (right) at the A/W interface.

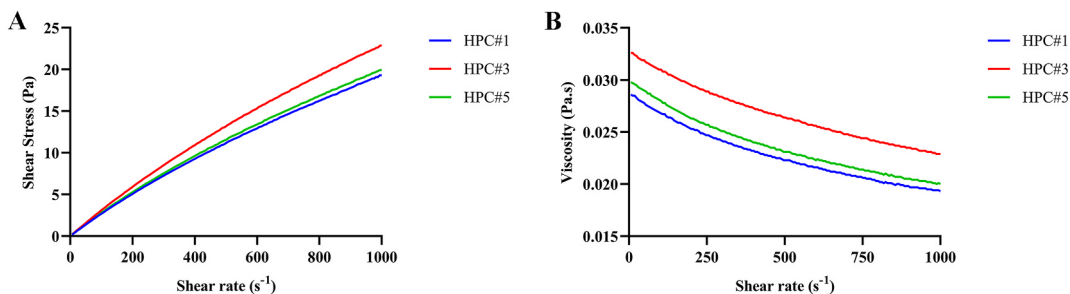


Fig. 8. Flow curves (A) and viscosity curves (B) of 1.0 wt% HPC solutions at 25 °C.

Table 4

Rheological parameters obtained from the Herschel-Bulkley model for 1.0 wt% HPC samples.

	HPC#1	HPC#3	HPC#5
n_0 (mPa.s)	28.57 ± 0.35^a	32.63 ± 0.21^c	29.75 ± 0.49^b
k (Pa.s ⁿ)	0.066 ± 0.002^a	0.073 ± 0.001^b	0.069 ± 0.003^{ab}
n (dimensionless)	0.824 ± 0.005^{ab}	0.833 ± 0.003^b	0.821 ± 0.004^a

n_0 : initial viscosity; k : consistency index; n : flow index. Within the same line, means with different letters are significantly different at $P \leq 0.05$.

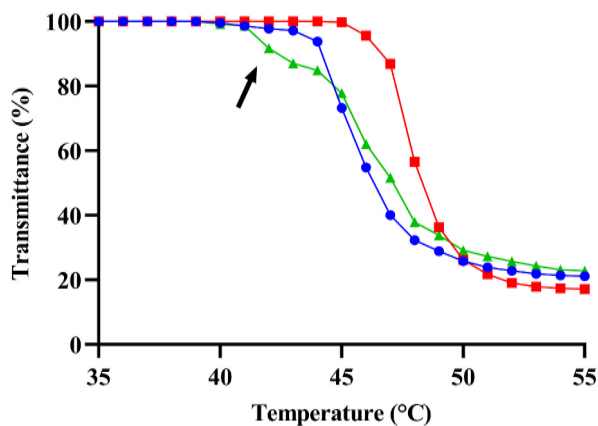


Fig. 9. Transmittance of 0.1 wt% HPC aqueous solution as a function of temperature: HPC#1 (●), HPC#3 (■), HPC#5 (▲) (heating rate = 0.2 °C/min).

would aggregate at higher temperatures. A strong correlation was observed between CP and surface hydrophobicity ($R^2 = 0.996$), which is not surprising as the clouding of HPC upon heating is the result of increasing hydrophobic interactions [51].

3.3. Structure-function relationship

Table 5 summarizes the different parameters evaluated and allows conclusions to be drawn about the impact of the structure on the

Table 5
Summary table of HPC physico-chemical properties and structural characteristics.

	HPC#1	HPC#3	HPC#5
MS	7.1	6.5	6.9
Released RS (mg/ml)	0.087 ± 0.002 ^a	0.119 ± 0.003 ^b	0.206 ± 0.004 ^c
Hydration rate (%)	83.0 ± 1.0 ^a	57.0 ± 14.0	94.0 ± 2.0 ^b
Eq. SFT (mN/m)	40.17 ± 0.07 ^a	43.90 ± 0.01 ^c	40.80 ± 0.01 ^b
Surface hydrophobicity	8.47 ± 0.24 ^a	7.72 ± 0.12 ^b	8.83 ± 0.22 ^a
Interfacial elasticity (mN/m)	4.99 ± 0.11 ^a	5.42 ± 0.40 ^a	7.44 ± 0.92 ^b
Viscosity (mPa.s)	28.57 ± 0.35 ^a	32.53 ± 0.21 ^c	29.75 ± 0.49 ^b
Cloud point (°C)	42.1 ± 0.1 ^b	46.0 ± 0.1 ^c	40.7 ± 0.1 ^a

Within the same line, means with different letters are significantly different at $P \leq 0.05$.

properties of these polymers. HPC#3 exhibited consistently shifted properties compared to HPC#1 and HPC#5. The structural characterization attributed this to a slightly lower substitution. The less pronounced substitution confers a greater hydrophilicity to this polymer, which greatly impacts the physico-chemical properties. The dispersion of HPC#3 in water requires considerably more time due to the formation of lumps. The polymer is less surface active, and gives more viscous solutions. Its lower hydrophobicity gives it greater thermal stability; more heating is required before the cloud point is reached, causing the polymer to precipitate.

HPC#5 had a more complex behavior; it has a similar MS compared to HPC#1 but differs by its more heterogeneous substitution profile. This atypical substitution pattern was shown to have only limited impact on the surface-activity and rheological properties of the polymer. However, the viscoelastic properties of a HPC-stabilized A/W interface were considerably affected. The higher dilatational moduli could be attributed to the combined effect of development of polymer-polymer interactions and conformation changes at the A/W interface following HPC adsorption. The greater substitution heterogeneity in HPC#5 had also a great impact on the phase behavior of the polymer, as illustrated by its bimodal clouding curve resulting in a lower CP value.

4. Conclusion

In conclusion, this work highlighted structural differences between HPC samples of the same technical specifications and studied their impact on the physico-chemical properties of the polymer. A wide range of properties, including water interaction, surface and rheological properties, and phase behavior were considered. The unusual behavior of HPC#5 was attributed to a more heterogeneous substitution pattern, with highly and weakly substituted regions distributed along the same polymer chain. This type of substituents distribution has already been observed for HPC [25], and other cellulose derivatives such as CMC [52,53] and HPMC [15,16]. The impact of a heterogeneous substitution profile on important functional properties of HPC, such as surface and rheological properties is reported for the first time. It was shown to greatly affect rheological behavior at the interface, and phase behavior of the polymer. The relationship between CP and MS has been established years ago; higher substituted celluloses are expected to have a lower CP [22,54]. Our results suggest that this relationship, although commonly accepted, is flawed. The structure-function relationship of such a compound cannot be studied by solely considering the number of substituents. Overall, this work emphasizes that beyond the absolute number of substituents, their distribution along the polymer chain is a critical factor determining their properties. Fine structural differences, not perceptible via the technical data sheet provided by suppliers, may exist and result in a different functionality. Compliance with the value range described in the commercial specifications is therefore not sufficient to guarantee identical functionality. Formulators should be aware of the existence, and consequences of such differences. This study provides new insights into the impact of structure on the functionality of HPC, and brings a valuable knowledge for any application using this polymer.

Author contribution statement

Gilles Cremer: Conceived and designed the experiments; Performed the experiments; Analyzed and interpreted the data; Wrote the paper. Sabine Danthine, Vera Van Hoed: Conceived and designed the experiments; Wrote the paper. Anne Dombree, Anne-Sophie Laveaux, Christian Damblon, Romdhane Karoui: Contributed reagents, materials, analysis tools or data. Christophe Blecker: Conceived and designed the experiments; Analyzed and interpreted the data; Wrote the paper.

Funding statement

This research did not receive any specific grant from funding agencies in the public, commercial, or not-for-profit sectors.

Data availability statement

Data will be made available on request.

Declaration of interest s statement

The authors declare no conflict of interest.

Appendix A. Supplementary data

Supplementary data to this article can be found online at <https://doi.org/10.1016/j.heliyon.2023.e13604>.

References

- [1] M.H. Godinho, D.G. Gray, P. Pieranski, Revisiting (hydroxypropyl) cellulose (HPC)/water liquid crystalline system, *Liq. Cryst.* 44 (12–13) (2017) 2108–2120, <https://doi.org/10.1080/02678292.2017.1325018>.
- [2] S. Mezdoor, G. Cuvelier, M.J. Cash, C. Michon, Surface rheological properties of hydroxypropyl cellulose at air-water interface, *Food Hydrocolloids* 21 (5–6) (2007) 776–781, <https://doi.org/10.1016/j.foodhyd.2006.09.011>.
- [3] Y. Takeuchi, K. Umemura, K. Tahara, H. Takeuchi, Formulation design of hydroxypropyl cellulose films for use as orally disintegrating dosage forms, *J. Drug Deliv. Sci. Technol.* 46 (2018) 93–100, <https://doi.org/10.1016/j.jddst.2018.05.002>.
- [4] K.M. Picker-Freyer, T. Dürig, Physical mechanical and tablet formation properties of hydroxypropylcellulose: in pure form and in mixtures, *AAPS PharmSciTech* 8 (4) (2007) 82–90, <https://doi.org/10.1208/pt0804092>.
- [5] A.H. Wander, B.H. Koffler, Extending the duration of tear film protection in dry eye syndrome: review and retrospective case series study of the hydroxypropyl cellulose ophthalmic insert, *Ocul. Surf.* 7 (3) (2009) 154–162, [https://doi.org/10.1016/S1542-0124\(12\)70310-5](https://doi.org/10.1016/S1542-0124(12)70310-5).
- [6] L. Zhang, H. Xia, F. Xia, Y. Du, Y. Wu, Y. Gao, Energy-saving smart windows with HPC/PAA hybrid hydrogels as thermochromic materials, *ACS Appl. Energy Mater.* 4 (9) (2021) 9783–9791, <https://doi.org/10.1021/acsaem.1c01854>.
- [7] T. Wuestenberg, Hydroxypropylcellulose, in: T. Wuestenberg (Ed.), *Cellulose and Cellulose Derivatives in the Food Industry: Fundamentals and Applications*, John Wiley & Sons Ltd., 2014, pp. 319–342, <https://doi.org/10.1002/9783527682935.ch07>.
- [8] H.C. Arca, L.L. Mosquera-Giraldo, V. Bi, D. Xu, L.S. Taylor, K.J. Edgar, Pharmaceutical applications of cellulose ethers and cellulose ether esters, *Biomacromolecules* 19 (7) (2018) 2351–2376, <https://doi.org/10.1021/acs.biomac.8b00517>.
- [9] T. Heinze, O.A. El Seoud, A. Koschella, Etherification of cellulose, in: *Cellulose Derivatives*, Springer, Cham, 2018, pp. 429–477, https://doi.org/10.1007/978-3-319-73168-1_6.
- [10] H.-P. Fink, D. Hofmann, H.J. Purz, Zur fibrillarstruktur nativer cellulose, *Acta Polym.* 41 (2) (1990) 131–137, <https://doi.org/10.1002/actp.1990.010410213>.
- [11] K. Mazeau, L. Heux, Molecular dynamics simulations of bulk native crystalline and amorphous structures of cellulose, *J. Phys. Chem. B* 107 (10) (2003) 2394–2403, <https://doi.org/10.1021/jp0219395>.
- [12] D. Klemm, B. Heublein, H.P. Fink, A. Bohn, Cellulose: fascinating biopolymer and sustainable raw material, *Angew. Chem. Int. Ed.* 44 (22) (2005) 3358–3393, <https://doi.org/10.1002/anie.200460587>.
- [13] T.C. Dahl, T. Calderwood, A. Bormeth, K. Trimble, E. Piepmeier, Influence of physico-chemical properties of hydroxypropyl methylcellulose on naproxen release from sustained release matrix tablets, *J. Contr. Release* 14 (1) (1990) 1–10, [https://doi.org/10.1016/0168-3659\(90\)90055-X](https://doi.org/10.1016/0168-3659(90)90055-X).
- [14] A. Viriden, B. Wittgren, T. Andersson, S. Abrahmsen-Alami, A. Larsson, Influence of substitution pattern on solution behavior of hydroxypropyl methylcellulose, *Biomacromolecules* 10 (3) (2009) 522–529, <https://doi.org/10.1021/bm801140q>.
- [15] A. Viriden, B. Wittgren, T. Andersson, A. Larsson, The effect of chemical heterogeneity of HPMC on polymer release from matrix tablets, *Eur. J. Pharmaceut. Sci.* 36 (4–5) (2009) 392–400, <https://doi.org/10.1016/j.ejps.2008.11.003>.
- [16] A. Viriden, A. Larsson, H. Schagerlöf, B. Wittgren, Model drug release from matrix tablets composed of HPMC with different substituent heterogeneity, *Int. J. Pharm.* 401 (1–2) (2010) 60–67, <https://doi.org/10.1016/j.ijpharm.2010.09.017>.
- [17] D. Desai, F. Rinaldi, S. Kothari, S. Paruchuri, D. Li, M. Lai, et al., Effect of hydroxypropyl cellulose (HPC) on dissolution rate of hydrochlorothiazide tablets, *Int. J. Pharm.* 308 (1–2) (2006) 40–45, <https://doi.org/10.1016/j.ijpharm.2005.10.011>.
- [18] Y. Sekiguchi, C. Sawatari, T. Kondo, A gelation mechanism depending on hydrogen bond formation in regioselectively substituted O-methylcelluloses, *Carbohydr. Polym.* 53 (2) (2003) 145–153, [https://doi.org/10.1016/S0144-8617\(03\)00050-X](https://doi.org/10.1016/S0144-8617(03)00050-X).
- [19] T. Kondo, The relationship between intramolecular hydrogen bonds and certain physical properties of regioselectively substituted cellulose derivatives, *J. Polym. Sci., Part B: Polym. Phys.* 35 (4) (1997) 717–723, [https://doi.org/10.1002/\(SICI\)1099-0488\(199703\)35:4<717::AID-POLB18>3.0.CO;2-J](https://doi.org/10.1002/(SICI)1099-0488(199703)35:4<717::AID-POLB18>3.0.CO;2-J).
- [20] H. Itagaki, M. Tokai, T. Kondo, Physical gelation process for cellulose whose hydroxyl groups are regioselectively substituted by fluorescent groups, *Polymer* 38 (16) (1997) 4201–4205, [https://doi.org/10.1016/S0032-3861\(96\)01007-5](https://doi.org/10.1016/S0032-3861(96)01007-5).
- [21] C. Alvarez-Lorenzo, J.L. Gomez-Amoza, R. Martínez-Pacheco, C. Souto, A. Concheiro, Interactions between hydroxypropylcelluloses and vapour/liquid water, *Eur. J. Pharm. Biopharm.* 50 (2) (2000) 307–318, [https://doi.org/10.1016/S0939-6411\(00\)00104-1](https://doi.org/10.1016/S0939-6411(00)00104-1).
- [22] E.D. Klug, Some properties of water-soluble hydroxyalkyl celluloses and their derivatives, *J. Polym. Sci. Part C: Polym. Symp.* 36 (1) (1971) 491–508, <https://doi.org/10.1002/polc.5070360137>.
- [23] A. Gomez-Carracedo, C. Alvarez-Lorenzo, J.L. Gomez-Amoza, A. Concheiro, Chemical structure and glass transition temperature of non-ionic cellulose ethers DSC, TMDSC®: oscillatory rheometry study, *J. Therm. Anal. Calorim.* 73 (2) (2003) 587–596, <https://doi.org/10.1023/A:1025434314396>.
- [24] S.A. Chang, D.G. Gray, The surface tension of aqueous hydroxypropyl cellulose solutions, *J. Colloid Interface Sci.* 67 (2) (1978) 255–265, [https://doi.org/10.1016/0021-9797\(78\)90010-3](https://doi.org/10.1016/0021-9797(78)90010-3).
- [25] H. Schagerlöf, S. Richardson, D. Momcilovic, G. Brinkmalm, B. Wittgren, F. Tjerneld, Characterization of chemical substitution of hydroxypropyl cellulose using enzymatic degradation, *Biomacromolecules* 7 (1) (2006) 80–85, <https://doi.org/10.1021/bm050430n>.
- [26] M. Martín-Pastor, E. Stoyanov, Mechanism of interaction between hydroxypropyl cellulose and water in aqueous solutions: importance of polymer chain length, *J. Polym. Sci.* 58 (12) (2020) 1632–1641, <https://doi.org/10.1002/pol.20200185>.
- [27] P. Taliq, U. Hubicka, The DSC approach to study non-freezing water contents of hydrated hydroxypropylcellulose (HPC): a study over effects of viscosity and drug addition, *J. Therm. Anal. Calorim.* 132 (1) (2018) 445–451, <https://doi.org/10.1007/s10973-017-6889-9>.
- [28] S.M. Mishra, A. Sauer, Effect of physical properties and chemical substitution of excipient on compaction and disintegration behavior of tablet: a case study of low-substituted hydroxypropyl cellulose (L-HPC), *Macromolecules* 2 (1) (2022) 113–130, <https://doi.org/10.3390/macromol2010007>.
- [29] A. Viriden, A. Larsson, B. Wittgren, The effect of substitution pattern of HPMC on polymer release from matrix tablets, *Int. J. Pharm.* 389 (1–2) (2010) 147–156, <https://doi.org/10.1016/j.ijpharm.2010.01.029>.
- [30] T.M. Wood, K.M. Bhat, Methods for measuring cellulase activities, *Methods Enzymol.* 160 (1988) 87–112, [https://doi.org/10.1016/0076-6879\(88\)60109-1](https://doi.org/10.1016/0076-6879(88)60109-1).
- [31] L. Segal, J.J. Creely, A.E. Martin, C.M. Conrad, An empirical method for estimating the degree of crystallinity of native cellulose using the X-ray diffractometer, *Textil. Res. J.* 29 (10) (1959) 786–794, <https://doi.org/10.1177/004051755902901003>.
- [32] H. Razafindralambo, C. Blecker, S. Delhaye, M. Paquot, Application of the quasi-static mode of the drop volume technique to the determination of fundamental surfactant properties, *J. Colloid Interface Sci.* 174 (2) (1995) 373–377, <https://doi.org/10.1006/jcis.1995.1404>.
- [33] A. Moro, C. Gatti, N. Delorenzi, Hydrophobicity of whey protein concentrates measured by fluorescence quenching and its relation with surface functional properties, *J. Agric. Food Chem.* 49 (10) (2001) 4784–4789, <https://doi.org/10.1021/jf001132e>.
- [34] Y.K. Erdem, Modification of casein micelle structure caused by ultrafiltration and heat treatment: a spectrofluorimetric and kinetic approach, *J. Food Eng.* 74 (4) (2006) 536–541, <https://doi.org/10.1016/j.foodeng.2005.03.041>.
- [35] M. Fettaka, R. Issaadi, N. Moulai-Mostefa, I. Dez, D. Le Cerf, L. Picton, Thermo sensitive behavior of cellulose derivatives in dilute aqueous solutions: from macroscopic to mesoscopic scale, *J. Colloid Interface Sci.* 357 (2) (2011) 372–378, <https://doi.org/10.1016/j.jcis.2011.02.041>.

- [36] F. Fitzpatrick, H. Schagerlöf, T. Andersson, S. Richardson, F. Tjerneld, K.G. Wahlund, et al., NMR, cloud-point measurements and enzymatic depolymerization: complementary tools for investigate substituent patterns in modified celluloses, *Biomacromolecules* 7 (10) (2006) 2909–2917, <https://doi.org/10.1021/bm060281o>.
- [37] P. Mischnick, J. Heinrich, M. Gohdes, O. Wilke, N. Rogmann, Structure analysis of 1,4-glucan derivatives, *Macromol. Chem. Phys.* 201 (15) (2000) 1985–1995, [https://doi.org/10.1002/1521-3935\(20001001\)201:15_1985::AID-MACP1985>3.0.CO;2-4](https://doi.org/10.1002/1521-3935(20001001)201:15_1985::AID-MACP1985>3.0.CO;2-4).
- [38] R.G. Zhbakov, Hydrogen bonds and structure of carbohydrates, *J. Mol. Struct.* 270 (1992) 523–539, [https://doi.org/10.1016/0022-2860\(92\)85052-I](https://doi.org/10.1016/0022-2860(92)85052-I).
- [39] W. Yao, Y. Weng, J.M. Catchmark, Improved cellulose X-ray diffraction analysis using Fourier series modeling, *Cellulose* 27 (10) (2020) 5563–5579, <https://doi.org/10.1007/s10570-020-03177-8>.
- [40] R. Talukder, C. Reed, T. Dürig, M. Hussain, Dissolution and solid-state characterization of poorly water-soluble drugs in the presence of a hydrophilic carrier, *AAPS PharmSciTech* 12 (4) (2011) 1227–1233, <https://doi.org/10.1208/s12249-011-9697-8>.
- [41] P. Wojciechowski, Thermotropic mesomorphism of selected (2-hydroxypropyl)cellulose derivatives, *J. Appl. Polym. Sci.* 76 (1999) 837–844, [https://doi.org/10.1002/\(SICI\)1097-4628\(20000509\)76:6_837::AID-APP9>3.0.CO;2-P](https://doi.org/10.1002/(SICI)1097-4628(20000509)76:6_837::AID-APP9>3.0.CO;2-P).
- [42] M. Kiyose, E. Yamamoto, C. Yamane, T. Midorikawa, T. Takahashi, Structure and properties of low-substituted hydroxypropylcellulose films and fibers regenerated from aqueous sodium hydroxide solution, *Polym. J.* 39 (7) (2007) 703–711, <https://doi.org/10.1295/polymj.PJ2006206>.
- [43] N. Bhatt, P.K. Gupta, S. Naithani, Hydroxypropyl cellulose from α -cellulose isolated from *Lantana camara* with respect to DS and rheological behavior, *Carbohydr. Polym.* 86 (4) (2011) 1519–1524, <https://doi.org/10.1016/j.carbpol.2011.06.054>.
- [44] M. Grossutti, J.R. Dutcher, Correlation between chain architecture and hydration water structure in polysaccharides, *Biomacromolecules* 17 (3) (2016) 1198–1204, <https://doi.org/10.1021/acs.biomac.6b00026>.
- [45] S. Aoki, H. Ando, M. Ishii, S. Watanabe, H. Ozawa, Water behavior during drug release from a matrix as observed using differential scanning calorimetry, *J. Contr. Release* 33 (3) (1995) 365–374, [https://doi.org/10.1016/0168-3659\(94\)00108-7](https://doi.org/10.1016/0168-3659(94)00108-7).
- [46] O. Mileti, N. Baldino, J.A. Carmona, F.R. Lupi, J. Muñoz, D. Gabriele, Shear and dilatational rheological properties of vegetable proteins at the air/water interface, *Food Hydrocolloids* 126 (2022), 107472, <https://doi.org/10.1016/j.foodhyd.2021.107472>.
- [47] E.M. Freer, K.S. Yim, G.G. Fuller, C.J. Radke, Interfacial rheology of globular and flexible proteins at the hexadecane/water interface: comparison of shear and dilatation deformation, *J. Phys. Chem. B* 108 (12) (2004) 3835–3844, <https://doi.org/10.1021/jp037236k>.
- [48] M.J. Cash, J. Caputo S, Cellulose derivatives, in: A. Imeson (Ed.), *Food Stabilisers, Thickeners and Gelling Agents*, Wiley-Blackwell, 2010, pp. 95–115, <https://doi.org/10.1002/9781444314724.ch6>.
- [49] P. Khuman, W.B.K. Singh, S.D. Devi, H. Naorem, Viscosity-temperature behavior of hydroxypropyl cellulose solution in presence of an electrolyte or a surfactant: a convenient method to determine the cloud point of polymer solutions, *J. Macromol. Sci., Pure Appl. Chem.* 51 (11) (2014) 924–930, <https://doi.org/10.1080/10601325.2014.953377>.
- [50] M. Gosecki, H. Setälä, T. Virtanen, A.J. Ryan, A facile method to control the phase behavior of hydroxypropyl cellulose, *Carbohydr. Polym.* 251 (2021), 117015, <https://doi.org/10.1016/j.carbpol.2020.117015>.
- [51] J. Gao, G. Haidar, X. Lu, Z. Hu, Self-association of hydroxypropylcellulose in water, *Macromolecules* 34 (7) (2001) 2242–2247, <https://doi.org/10.1021/ma001631g>.
- [52] B. Saake, S. Horner, T. Kruse, J. Puls, T. Liebert, T. Heinze, Detailed investigation on the molecular structure of carboxymethyl cellulose with unusual substitution pattern by means of an enzyme-supported analysis, *Macromol. Chem. Phys.* 201 (15) (2000) 1996–2002, [https://doi.org/10.1002/1521-3935\(20001001\)201:15_1996::AID-MACP1996>3.0.CO;2-X](https://doi.org/10.1002/1521-3935(20001001)201:15_1996::AID-MACP1996>3.0.CO;2-X).
- [53] J. Kötz, I. Bogen, T. Heinze, U. Heinze, W.M. Kulicke, S. Lange, Peculiarities in the physico-chemical behaviour of non-statistically substituted carboxymethylcelluloses, *Colloids Surf., A* 183–185 (2001) 621–633, [https://doi.org/10.1016/S0927-7757\(01\)00518-0](https://doi.org/10.1016/S0927-7757(01)00518-0).
- [54] L. Robitaille, N. Turcotte, S. Fortin, G. Charlet, Calorimetric study of aqueous solutions of (Hydroxypropyl)cellulose, *Macromolecules* 24 (9) (1991) 2413–2418, <https://doi.org/10.1021/ma00009a044>.